THERMIC BEHAVIOUR SPINDLE OF MACHINE TOOLS

Marian-Cornel CEAUSESCU[1], Cleopatra CEAUSESCU[2], Mădălina CIUPITU[3], Claudiu Florinel BISU[4]

Rezumat. *Anticiparea comportamentului termo-mecanic al arborelui maşinii-unealtă este esențial în funcționarea fiabilă a maşinilor-unealtă la viteze foarte mari. În particular, performanța la turații înalte ale arborelui principal este dependentă de comportamentul termic al acestuia. Principala sursă de generare de caldură a arborelui este cuplul de frecare în rulmenții cu bile de contact unghiular.*

Abstract. *The prediction of the thermo-mechanical behaviour of machine-tool spindles is essential in the reliable operation of high speed machine tools. In particular, the performance of these high speed spindles dependents on their thermal behaviour. The main source of heat generation in the spindle is the friction torque in angular contact ball bearings.*

Keywords: thermic, mechanical, spindle, high speed, machine-tools.

1. Introduction

Machining, in general, remains a major manufacturing process in various industries. Almost all metal parts undergo machining at some stage of their production. High speed and high precision machine tools have become a major trend of machining industries in recent years.

The performance and reliability of these machines are also influenced by the high speed spindles that are essential to the process. High speed spindles are known to suffer from lack of reliability and sudden failure, which derives, mostly, from thermal loads. In order to ensure the reliable operation of spindles, it is necessary to predict the thermo-mechanical behaviour of high speed spindles. The major sources of heat in a spindle system are contact forces at bearings and the friction force with an environmental air and rotor/stator in motorized spindles. Angular contact ball bearings are the most commonly used types of bearing in machine tools. These bearings are usually subjected to preloads, in addition to externally

[1] Eng. Marian-Cornel CEAUSESCU, Engineering and Management of Technological Systems, Politehnica University of Bucharest, Romania (ceausescumariancornel@yahoo.com).
[2] Eng. Cleopatra CEAUSESCU, Engineering and Management of Technological Systems, Politehnica University of Bucharest, Romania (cleopatra.ceausescu@yahoo.com).
[3] Eng. Mădălina CIUPITU, Engineering and Management of Technological Systems, Politehnica University of Bucharest, Romania.
[4]As. Prof. Dr. Eng. Claudiu Florinel BISU Engineering and Management of Technological Systems, Politehnica University of Bucharest, Romania.

applied loads, to obtain the required stiffness. Thermal loads cause the preload to vary, creating a thermal preload. Heat generation in angular contact ball bearings occurs due to three phenomena: load-related, viscosity-related and spin-related heat generation. Since the mechanical and thermal characteristics of a spindle system have a mutual effect on each other, the accurate thermo-mechanical modelling of ball bearings and the spindle shaft are essential in predicting the spindle response to mechanical and thermal load, and will help in designing more reliable spindles.

A micro-milling spindle differs significantly from a larger spindle. The differences are not only in relative size and power consumption but also in maximum speeds and distribution of its power between the cutting process and the power needed to overcome the friction of a spindle's bearings. Since the maximum speed of a micro-milling spindle is generally higher than its larger counterpart, this growth effect is expected to be relatively more significant for a high-speed micro-milling spindle.

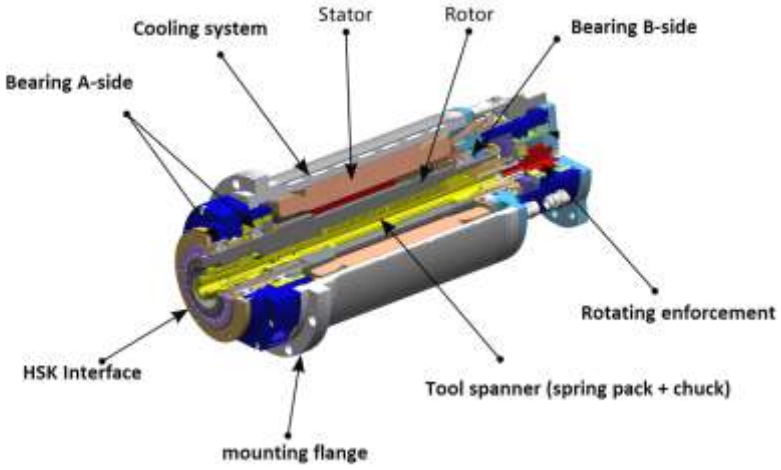

Fig. 1. Motorized spindle [1].

Additionally, in a larger spindle used in macro-machining most of the spindle power is used for cutting. However, in micro-machining only a small percentage of the spindle's power is used for cutting; the rest is used to overcome the friction in its bearings. Hence a significant portion of the spindle thermal growth occurs during the heat generated to overcome this friction. This portion of the spindle growth can be effectively counteracted by capturing the spindle deformation while running the spindle in free-air and developing a compensation scheme based on those growth values.

The parts of the spindle are supported by two sets of angular contact ceramic ball in front and one set of angular contact ceramic ball bearing in the rear which is installed back to back. The motor is set between the front second set and the rear bearings. As one whole body, the stator and the coolant jacket are installed to the shell of the spindle. Two lock nuts are used to give preload. One lock nut is positioned at the second set of the second set of the front bearing with front preload spacer.

Another one is placed at the rear set of the bearings with a rear preload spacer. Front and rear bearing housing are placed over the bearing system. The coolant jacket is placed over the stator-rotor system and the outer body is placed over the coolant jacket. The front spindle, the front and back bearing system, the stator-rotor system coolant jacket are shown in Figure 1 and the outer body is only considered in the high speed motorized spindle in both thermal and vibration analysis. The sensor ring and the servo controller of the high speed motorised spindle are not included in either analyses.

The mode shapes and damping factors of the structures were calculated using the results of the Fast Fourier Transform of the vibration signals from the accelerometer. By using the half-power band with method, we can find the damping factor of the spindle from the response curve:

$$\eta = \P_2 - f_1 \perp f_r, \tag{1}$$

where $(f_2 - f_1)$ and f_r represent the half power band width and the corresponding natural frequency. The damping ratio of the spindle is 0,060.

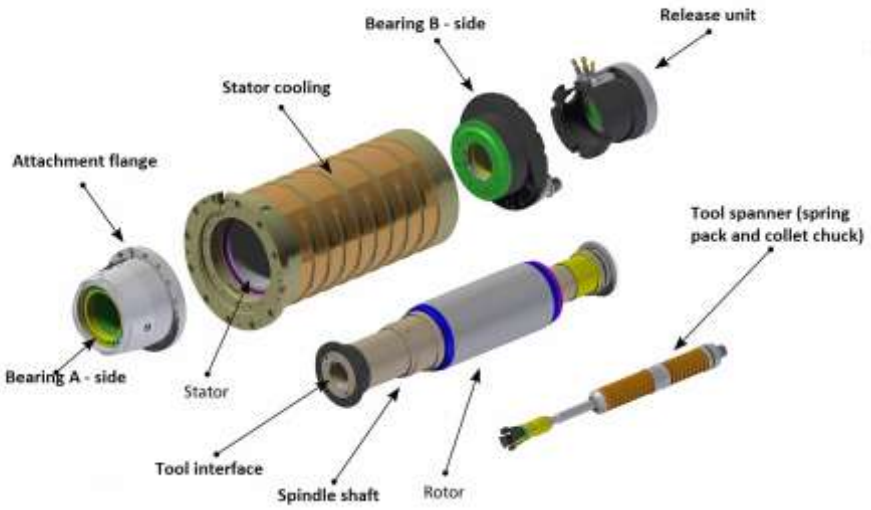

Fig. 2. Motorized **s**pindle components [1]

Finally, the smaller spindles used for micro-milling are generally air cooled, since they do not have enough real-estate for installation of effective liquid-cooling channels. Since liquid cooling has a higher heat capacity compared to similarly sized air-cooling channels, these micro-milling spindles may grow significantly even in the presence of cooling, thus necessitating a presence of a growth compensation scheme.

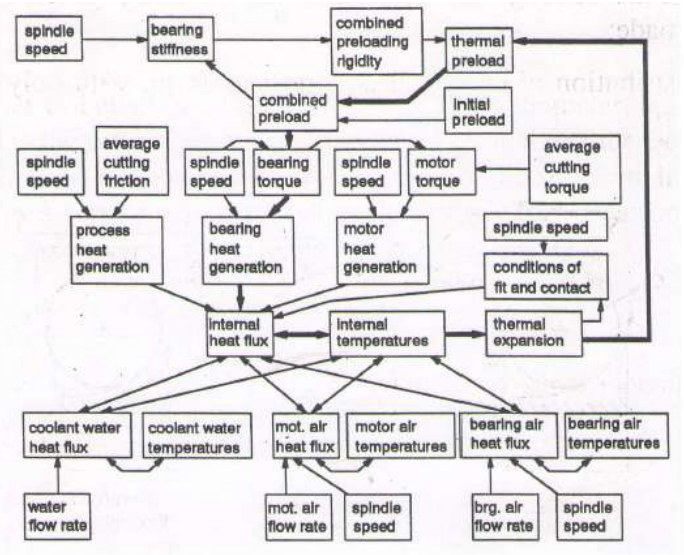

Fig. 3. The cause-effect heat transfer in a motor-spindle [2]

2. Heat transfer model

The heat exchange model was based on the following features (Fig. 3):

• the main sources of heat are the cutting process, the friction of the electric motor and friction bearings;

• electricity engine partially converted into heat (losses in the primary coil of copper, internal losses, losses in the auxiliary coil of copper), stator and rotor transfer;

• part of the transformed electric energy into mechanical energy participating in overcoming viscous friction of the air surrounding the engine (loss through friction with air), friction in the bearings;

• on the other hand thermal expansion is dependent on the generation of heat forming a closed cycle of cause and effect;

• increasing tension in the camps still producing heat generation due to friction in the camp, they can be super tensed, which contributes to excessive wear and hence a thermal galling.

Governing equations. In the model heat transfer from Fig. 3, is established the meshing of the assembled structured spindle-motor: • each model element has only one degree of freedom, which is its average temperature, located in its geometrical centre; • heat flux is transmitted through the common contact zone from a central node to the neighbouring nodes centre; • for convection it is assumed that the temperatures of the surface are close temperatures of central elements and that the temperature difference between the surface and the cooling liquid replaced convective heat flow; • through coaxial and cylindrical elements (Fig. 4), the heat transfer is produced through conduction, the heat balance equation becoming:

$$\dot{q}_e + \dot{q}_i + \dot{q}_a + \dot{q}_p + \dot{q}_n = c_1 \frac{dT}{dt}. \tag{1}$$

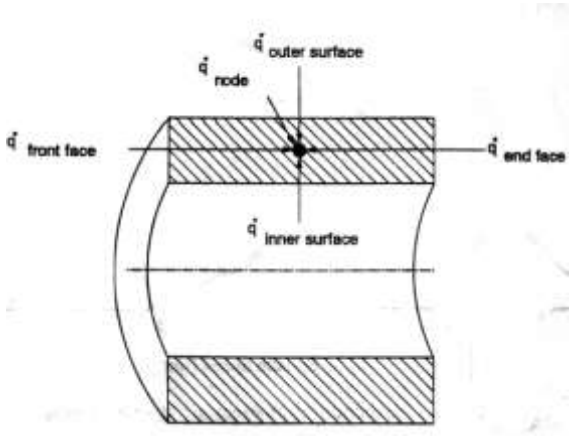

Fig. 4. Element of heat transfer.

where: $\dot{q}$ is the density of the heat flow; indices e, i, a, p, in this order referring to the outer surface of the element, inner surface, the previous front surface, the posterior front surface and respectively the surface of the node element.

3. Internal Heat Transfer Mechanisms

3.1. Heat transfer through bearings. Within this heat transfer, convective heat exchange is prevalent. Simplifying assumptions as significant are:

• the temperature distribution of each bearing is considered uniform, although there are hot and cold points on the surface of contact between bodies and the raceways of the inner and outer rings;

• uniform temperature inside the bearing;

• all bearings have the same temperature as rotate with angular speeds so high that the flow of heat is distributed evenly;

• the contact surfaces between the bodies and the raceways, the temperature is identical, the temperature variation occurring at the spindle and to the housing;

• heat transfer is neglected in lubricating oil between the bodies and raceways

• heat transfer radially through the gap between the outer ring and housing changes according to the average linear size of the gap;

• the existence of a loose-fitting between the outer ring and the housing which requires calculations in detail for heat transfer;

• instead, due to the interference fit between the inner ring and spindle shaft, the contact thermal resistance can be modelled by a constant value.

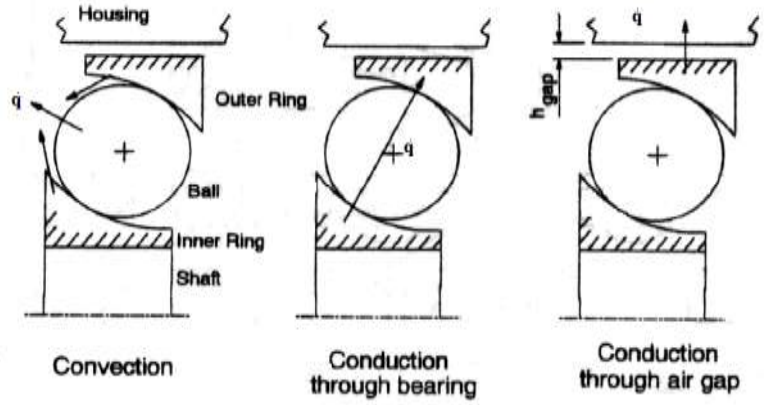

Fig. 5. Heat transfer through bearings [13].

3.2. Convection by lubrication air. The oil-air lubrication for the motor spindle-shaft bearings require a very small quantity of oil (typically 0.15 ml every 2 minutes) with an air flow of 2.5×10^{-3} m^3/s. For this reason, it is assumed that the heat transfer is performed by forced air convection, the heat flux is absorbed within a bearing being:

$$A_{cv} = A_{cr\ i} + z \cdot A_r + A_{cr\ e} = \frac{\pi^2}{2} \cdot d_{med} \cdot \rho_i + z \cdot \pi \cdot d_r^2 + \frac{\pi^2}{2} D_{med} \cdot \rho_e \tag{2}$$

where: $A_{c\ ri}$ and $A_{cr\ e}$ is the surface area of the inner ring of the driveway, respectively, of the outer ring; z – number of balls; A_r – the surface area of the ball; d_{med} and D_{med} – the average diameter of the inner ring respectively outer ring; ρ_i and ρ_e – race of curvature of the raceway of the inner ring corresponding, respectively, to the outer ring. The average speed of the air bearings is obtained by the superposition of the axial and tangential velocity in the direction of air flow.

$$\bar{u} = \left(\left(\frac{\dot{v}_a}{A_{ax}} \right)^2 + \left(\frac{\pi \cdot n \cdot \frac{D_{med} + d_{med}}{2}}{2} \right)^2 \right)^{1/2} \tag{3}$$

where $A_{ax} = \pi \left(D_{med}^2 - d_{med}^2 \right) / 4$ is the surface area of the axial air flow between the inner and outer raceways; n – spindle speed; $\dot{v}_a$ – volumetric air flow stream. The coefficient of convective heat exchange can be determined by a simple polynomial function having this form:

$$\alpha_{cv} = c_0 + c_1 + u^{-c_2} \text{ [W / (m}^2 \times \text{K]} \tag{4}$$

where c_0, c_1 and c_2 are the constants to be determined experimentally [4]. The spindle speed for different values of the motor has shown the characteristic coefficient of convection air bearing lubrication according to the flow prior to the air bearing (in terms of atmospheric pressure).

3.3. Conduction between balls and raceways. For this purpose, the contact thermal resistance is defined by conduction R_t based on the fundamental principles of Harris [15] and Nakajimap. This parameter of heat transfer depends on the shape and size of the contact, in its turn depending on the geometry of the bearing and the strength of its internal contact. Relate to half the surface area of contact

$$R_t = \frac{1}{4\pi \cdot \lambda} \int_0^{\infty} \frac{du}{\sqrt{\left(a^2 + u \right)\left(b^2 + u \right) u}} \quad \text{[m}^2 \times \text{K)/W]} \tag{5}$$

where λ is the thermal conductivity in W/(m×K) reported at half the surface area of contact; a, b – semi-axes of the ellipse of contact ($a > b$).

$$R_t = \frac{\psi}{4\lambda \cdot a}, \tag{6}$$

where ψ is a geometrical factor depending on the size of the contact surface as the coefficient $k = 1 - b^2/a^2$.

$$\psi = \frac{2}{\pi} \int_0^{\pi/2} \frac{d\theta}{\sqrt{\left(1 - k^2 \cdot \sin^2 \theta \right)^{1/2}}} \tag{7}$$

For a ball bearing, the contact thermal resistance to the outer ring becomes:

$$\bar{R}_{t0} = \frac{\psi}{4a} \left(\frac{1}{\lambda_1} + \frac{1}{\lambda_2} \right) \tag{8}$$

where λ_1 and λ_2 is the thermal conductivity outside the ring and ball, respectively. Taking into account the z balls of a bearing, then:

$$R_{t0} = \overline{R}_{t0} / z \tag{9}$$

Further we determined: the conduction between outer bearing rings and housing, the heat transfer from the spindle structure into fluids, the convection of the cooling water, and the convection of the ambient air.

4. Model Description

The heat is mainly generated at bearing raceways and balls due to the friction influenced by speed, preload and lubricant; the bearing temperature distribution rises due to the heat generated by friction losses [5]. The equation gives the heat in the bearing.

$$N_R = \frac{M_R \cdot n}{9500}. \tag{10}$$

The total friction of a ball bearing under preload, lubricant and speed conditions is given by the sum of the load torque and viscous friction torque.

$$M_R = M_0 + M_1 \tag{11}$$

In the following equation M_0 is the viscous friction torque as a function of speed and can be expressed as (1):

$$M_0 = 10^{-7} f_0 \cdot (v \cdot n)^{\frac{2}{3}} d_m^3 \qquad v \cdot n \geq 2000 \tag{12}$$

$$M_0 = 160 \cdot 10^{-7} f_0 \cdot d_m^3 \qquad v \cdot n \leq 2000 \tag{13}$$

where parameter f_0 is a factor depending on the bearing and lubrication type, and for the angular contact ball bearing $f_0 = 2$, v is the kinematics viscosity of lubricant at operation temperature.

M_1 is the load torque of the mechanical friction and is a function of load for ball bearings with spherical roller:

$$M_1 = f_1 \cdot P_1 \cdot d_m \tag{14}$$

f_1 is a bearing factor for frictional torque as a function of preload, P_1 depends on the value and direction of the load, d_m is the mean bearing diameter.

For angular contact ball bearing:

$$f_1 = 0{,}001\left(\frac{P_0}{C_0}\right) \tag{15}$$

for single bearing

$$P_1 = F_a - 0{,}1 \cdot F_r \tag{16}$$

for bearing pair

$$P_1 = 1{,}4 \cdot F_a - 0{,}1 \cdot F_r \tag{17}$$

where: C_0 is basic rating static load, P_0 is equivalent static radial load, F_a axial load and F_r radial load.

$$P_0 = X_s \cdot F_r - Y_s \cdot F_a \tag{18}$$

where: X_s and Y_s values for the single row angular contact ball bearing with different contact angles are given in Table 1.

Table 1 values X_s and Y_s for angular contact ball bearings.

Table 1

Contact angle	**15^0**	**20^0**	**25^0**	**30^0**	**35^0**
X_s	0.58	0.5	0.5	0.5	0.5
Y_s	0.47	0.42	0.38	0.33	0.29

Conclusions

A novel method is proposed for designing the headstock structure for NC lathe with minimized thermal displacement in X direction using CAE techniques. With the proposed design method, an optimal headstock design immune to thermal displacement was possible after analyzing only 18 patterns, which dramatically reduce the development time and cost comparing to the traditional trial and error approach.

Dynamically simulate and analyze the thermal behaviour such as the temperature field and thermal deformation of the spindle. In addition, a novel method for selecting the thermal key points was proposed. Finally, a verification experiment implemented on this turning centre showed that the simulation results were satisfying to replace the experiment data, which has a great significance in reducing the production costs and increasing the efficiency.

REFERENCES

[1] Anton Mayer, *Effizienzsteigerung bei Werkzeugspindeln*, Ressourceneffizienz – Chancen, Technologien und Rahmenbedingungen, 60 Jahre VDMA Baden-Württemberg, 2003.

[2] B. Bossmanns, J. F.Tu, *Thermal Model for High Speed motorized Spindles*, International Journal of Machine Tools and Manufacture, 39 (9) (1999) 1345-1366.

[3] Charles Wang Bob Griffin, *A Noncontact Laser Technique for Circular Contouring Accuracy Measurement*, Review of Scientific Instruments 72 (2001) 1594-1596.

[4] D.A. Krulewich, *Temperature Integration Model and Measurement Point Selection for Thermally Induced Machine Tool Errors*, Mechantronics 8 (1998) 395-412.

[5] Emil Udup, Claudiu Florinel Bisu, Miron Zapciu, *Numerical Model for Thermo-Mechanical Spindle Behavior*, National Institute of Physics and Nuclear Engineering.

[6] J.S. Chen, G. Chiou, *Quick Testing and Modeling of Thermally Induced Errors of CNC Machine Tools*, International Journal of Machine Tools and Manufacture 35 (7) (1995) 1063-1074.

[7] Jin-Hyeon Lee, Seung-Han Yang, *Statistical Optimization and Assessment of a Thermal Error Model for CNC Machine Tools*, International Journal of Machine Tools and Manufacture 42 (2002) 147-155.

[8] Jianguo Yang, Jingxia Yuan, Jun Ni, *Thermal Error Mode Analysis and Robust Modeling for Error Compensation on a CNC Turning Center*, International Journal of Machine Tools and Manufacture 35 (1999) 1367-1381.

[9] N. Srinivasa, J.C. Ziegert, *Automated Measurement and Compensation of Thermally Induced Error Maps in Machine Tools*, Precision Engineering 19 (1996) 112-132.

[10] N. Srinivasa, J.C. Ziegert, C.D. Mize, *Spindle Thermal Drift Measurement Using the Laser Ball Bar*, Precision Engineering 18 (1996) 118-128.

[11] P. Vanherck, J. Dehaes, M. Nuttin, *Compensation of Thermal Deformations in Machine Tools with Neural Nets*, Computers in Industry 19 (1996) 112-132.

[12] Seung-Han Yang, Ki-Hoon Kim, Yong Kuk Park, *Measurement of Spindle Thermal Errors in Machine Tool Using Hemispherical Ball Bar Test*, International Journal of Machine Tools and Manufacture 44 (2004) 333-340.

[13] Ting-Yu Chen, Wei-Jiunn Wei, Jhy-Cherng, *Optimum Design of Headstocks of Precision Lathes*, International Journal of Machine Tools and Manufacture 39 (1999) 1961-1977.

[14] Tae Jo Ko, Tae-weon Gim, Jae-yong Ha, *Particular Behavior of Spindle Thermal Deformation by Thermal Bending*, International Journal of Machine Tools and Manufacture 43 (2003) 17-23.

[15] T.A. Harris, *Rolling Bearing Analysis*, Wiley, New York, 1991 (pp. 540-560).